20. Ketterling, J. A. & Apfel, R. E. Experimental validation of the dissociation hypothesis for single bubble sonoluminescence. *Phys. Rev. Lett.* **81,** 4991–4994 (1998).
21. Zel'dovich, Y. B. & Raizer, Y. P. *Physics of Shock Waves and High-Temperature Hydrodynamic Phenomena* Vols I & II (Academic, New York, 1966).
22. Fyrillas, M. M. & Szeri, A. J. Dissolution or growth of soluble spherical oscillating bubbles. *J. Fluid Mech.* **277,** 381–407 (1994).
23. Holt, G. & Gaitan, F. Observation of stability boundaries in the parameter space of single bubble sonoluminescence. *Phys. Rev. Lett.* **77,** 3791–3794 (1996).
24. Prosperetti, A. & Hao, Y. Modeling of spherical gas bubble oscillations and sonoluminescence. *Phil. Trans. R. Soc. Lond.* **357,** 203–224 (1999).

Supplementary information is available on *Nature*'s World-Wide Web site (http://www.nature.com) or as paper copy from the London editorial office of *Nature*.

Acknowledgements. We thank S. Koehler, W. Moss and H. Stone for discussions. Support by the DFG and partial support by the NSF is acknowledged.

Correspondence and requests for materials should be addressed to D.L. (e-mail: lohse@tn.utwente.nl).

Immobility of protons in ice from 30 to 190 K

J. P. Cowin*, A. A. Tsekouras†, M. J. Iedema*, K. Wu* & G. B. Ellison‡

* *Pacific Northwest National Laboratory, Box 999, MS K8-88, Richland, Washington 99352, USA*
† *Laboratory of Physical Chemistry, University of Athens, Athens GR-15771, Greece*
‡ *Department of Chemistry & Biochemistry, University of Colorado, Boulder, Colorado 80309, USA*

The anomalously fast motion of hydronium ions (H_3O^+) in water is often attributed to the Grotthuss mechanism[1,2], whereby protons tunnel from one water molecule to the next. This tunnelling is relevant to proton motion through water in restricted geometries, such as in 'proton wires' in proteins[3] and in stratospheric ice particles[4]. Transport of hydronium ions in ice is thought to be closely related to its transport in water[1,2]. But whereas claims have been made that such tunnelling can persist even at 0 K in ice[5–7], counter-claims suggest that the activation energy for hydronium motion in ice is non-zero[8–10]. Here we use 'soft-landing'[11–13] of hydronium ions on the surface of ice to show that the ions do not seem to move at all at temperatures below 190 K. This implies not only that hydronium motion is an activated process, but also that it does not occur at anything like the rate expected from the Grotthuss mechanism. We also observe the motion of an important kind of defect in ice's hydrogen-bonded structure (the D defect). Extrapolation of our measurements to 0 K indicates that the defect is still mobile at this temperature, in an electric field of 1.6×10^8 V m^{-1}.

Water's hydrogen-bonded network must be disrupted to solvate or transport ions. Figure 1 shows the hydrogen bonding in a thin film of water. Normally, each water molecule hydrogen-bonds with four neighbours. Three hydronium ions were initially placed on top of the film. At right, a proton has hopped four monolayers down, via the Grotthuss mechanism. Figure 1 shows D and L defects, which are misdirected hydrogen bonds, that put either two or zero protons between two adjacent oxygens instead of the usual one proton. These D/L defects facilitate the re-orientation of water molecules, creating water's high solvation power and dielectric constant ϵ.

The ions in Fig. 1 will move in their collectively self-generated electric field $|E|$. When all ions are at the top of a film (of thickness b) on an earthed substrate, this gives a 'film voltage' ΔV of

$$\Delta V = |E|b = \frac{Qb}{A\epsilon\epsilon_0} \quad (1)$$

where charge Q is deposited over area A, and ϵ_0 is the vacuum permittivity. The ion motion could be measured by the time-dependent current induced between an electrode placed on top of the film and the substrate, as in the classical 'proof' of proton tunnelling, the 95–180 K study by Eckener *et al.*[5] They used 0.5-J laser pulses to "stimulate" the release of hydronium ions from hydrogen-gas-pretreated Pd powder. The powder was pressed onto one face of ice crystal wafers 90–300 μm thick; the opposing face was a biased electrode. However, these difficult experiments (never duplicated) are prone to artefacts[10,14]. "Proton injection" experiments at much higher temperatures also claim a zero activation

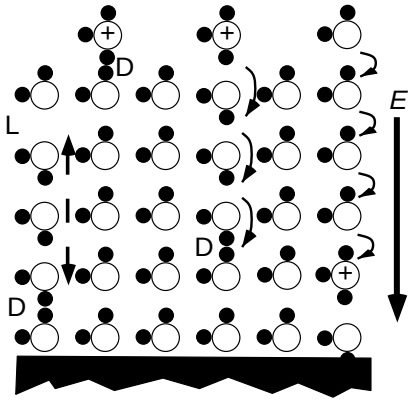

Figure 1 Ice structure and transport. A diagram of ice's hydrogen-bonding network is shown. On top were placed three hydronium ions (+). L and D hydrogen-bond defects are also present. At the top, 'soft-landed' hydronium ions form D defects. At right the hydronium ion's proton, in an electric field E, has hopped to an adjacent water four times, changing the hydronium's position. In the centre, a D defect moves away from the hydronium. At left, an L/D-defect pair formed and diffused apart.

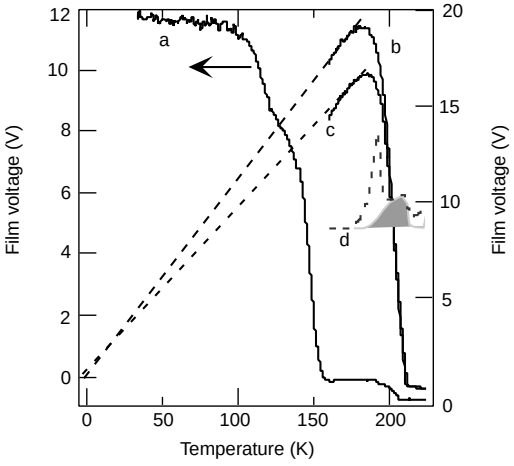

Figure 2 Lack of diffusion of hydronium ions in water ice. Data are shown for crystalline water films dosed with hydronium ions. Trace a, 2,880 monolayers (ML) grown at 150 K, ion-dosed (20 nC) at 33 K. Voltage (left axis) is shown as temperature T is increased at 0.167 K s^{-1}. Trace b, 5,980 ML grown at 165 K, then ion-dosed (700–3,800 nC) at 165 K. Trace c, 820 ML dosed at 165 K, ion dosed (600–1,900 nC) at 165 K, then water dosed (480 ML) at 165 K. (Traces b, c use right axis.) Water desorption occurs near 200 K for these thick films (trace d, shown for 5,980 ML film). Maximum ion dose is 2.6% of a monolayer. The water desorption curve is double-peaked, as the Kelvin probe slows desorption from the region behind it. The shaded portion is the desorption peak to compare to the work-function changes. ϵ was measured to be about 2.3 ± 33% for the start of trace a, and 160 (±50%) for the start of curves b and c. Voltage remaining high from 33 to 150 K (trace a) and from 160 to 190 K shows that hydronium ions do not move in these temperature ranges. Dashed curve is the expected behaviour from equation (1), for ϵ proportional as $1/T$, if hydronium ions do not move.

© 1999 Macmillan Magazines Ltd

barrier (ref. 6, and ref. 7 and refs therein). But like Eckener *et al.*, these higher temperature experiments probably produced mixtures of hydronium ions, counter-ions, D/L defects and even H_2. Measurements using infrared spectroscopy and NMR indicate activation barriers of ~0.4 and 0.1 eV (refs 8, 9, 15), but distances were ill-defined, planar defects and traps were present, and counter-ions were produced.

To overcome these limitations, we gently "soft-landed"[11–13,16] pure hydronium ions from our mass-selected 1-eV source onto ultrathin ice films. We do not use counter-ions; this is an advantage, as they interfere badly when determining ion mobility. We have used 'soft-landed' ions to probe ion diffusion in glassy hydrocarbon films[17]. These simpler systems allowed comparison with ion mobilities estimable from published viscosities; the good agreement validated our method (see Supplementary Information).

The film voltage ΔV in equation (1) changes the work function by $-\Delta V$, which is measurable by a non-contacting Kelvin probe[18]. If ϵ is roughly constant, then the work function measures the motion of the ions; b in equation (1) is replaced by the average ion height $\langle z \rangle$. ϵ varies slowly for ice at temperature $T > 160$ K. Then ϵ is "active" (that is, the time τ for reorientating water dipoles is $\leqslant 1$ s), and equals about (27,000 K)/T (ref. 1). Below 130 K $\tau \gg 1$ s, so ϵ then is constant at ~3.2.

We prepared targets by depositing D_2O or H_2O films, 0.2–1.5 μm thick, on a Pt(111) single crystal, yielding single-crystal ice above 140 K (ref. 19). The ion beam energy is kept to 1 eV during ion deposition by adjusting the target voltage to compensate for the film voltage.

Figure 2 shows ΔV for D_3O^+ ions initially deposited on D_2O ice at 33 K. The initial film voltage is 11.7 V for 20 nC deposited ions. The calculated ϵ via equation (1) is 2.3 ± 33% assuming that the ions stay on top of the film. Significant ion motion would decrease the calculated ϵ, moving it unreasonably far from the established value of 3.2 (ref. 1). Thus hydronium ions do not move at 33 K, even in a 1.1×10^7 V/m field.

Figure 2 trace a shows as that, the temperature is ramped, the film voltage stays nearly constant up to 100 K, then drops in steps at 110, 150 and 200 K. Near 150 K ϵ should become "active", increasing to over 100, accounting for this large voltage drop. Substantial water desorption begins around 180 K. The drop at 200 K is caused by desorption of the last of the water, and a work function change of +0.6 V. The lack of large voltage changes below 150 K shows that hydronium ions do not move from 33 to 120 K, and probably to 150 K.

To probe hydronium-ion motion above 150 K, we deposited substantially more ions, at temperatures between 140 and 165 K, where the dielectric constant is large. Data for H_2O ice grown at 165 K are given in Fig. 2 traces b and c. Equation (1) shows that, if the ions do not move, the voltage should vary as $1/\epsilon(T)$. For $T \geqslant 160$ K, ϵ varies as $1/T$, predicting a voltage proportional to T. Figure 2 shows the work function does increase linearly with T, until water desorption near 200 K. Thus hydronium ions do not move in ice from 33 to 190 K.

One concern is that there may be a surface trap or barrier preventing the ions from entering the ice bulk. We sandwiched ions inside crystalline ice films (Fig. 2 trace c), and saw no evidence of any surface trap: thus the non-mobility of the hydronium ions is a true bulk ice effect. The data in Fig. 2 are for D_3O^+ reported on both D_2O and H_2O. As exchange is facile above 160 K (refs 8, 9), no mobility occurs for either D_3O^+ in D_2O or H_3O^+ in H_2O.

The absence of the Grotthuss mechanism is easy to rationalize. Tunnelling over long distances should only occur if the potential is periodic. But normal ice is proton-disordered[1], thereby destroying the periodicity. Further, the hydronium ions should self-trap in a polarization well. A hydronium ion will force nearby water molecules to reorientate, pointing away their hydrogen ends. If the proton tries to move without the polarization pattern following it, it finds a deep well that it cannot escape. Solvation well effects have been surmised to occur elsewhere, as in calculated proton motions[20], or polaron trapping near −40 °C (ref. 21).

Other experimenters[8,9] have deduced that activated hydronium-ion motion in fact occurs at 140 or 115 K, rather than above 190 K as we find. We speculate that mobile D/L defects lower the activation barrier for hydronium–hydroxide ion-pair formation, permitting transient local ion pairs. This mimics hydronium-ion transport.

Figure 2 trace a shows a drop in ΔV near 110 K, where D/L defects should become mobile[1]. The voltage always drops by about 0.3 to 0.5 times its initial value, as shown in Fig. 3 at various fields, and for a variety of other conditions (not shown). This is due to motion of D defects generated by the ions themselves: one D defect per hydronium ion. As in Fig. 1, each hydronium ion is expected to create D defects, owing to its extra proton and its weakly complexing oxygen end[1]. Creation of a D/L defect pair requires[1] about 0.68 eV, so natural D/L defect concentrations should be insignificant below 150 K. The D/L defects have an effective charge of $\pm(0.38\, q_e)$,

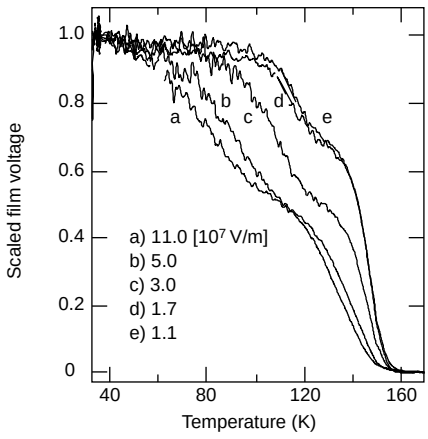

Figure 3 Evidence for hydrogen-bond defect motion. Shown is film voltage versus T for ions placed on crystalline water at various electric fields. The data has been scaled to the initial bias (with zero taken near 180 K to eliminate the 0.6 V work-function change from the first monolayer). Ice was grown at 150 K, ions dosed near 30 K. The rate of temperature increase is 0.167 K s^{-1}. Trace a, 600 ML D_2O, 24 V initial voltage; trace b, 1440 ML, 26 V; trace c, 2,780 ML, 30 V; trace d, 5,060 ML, 32 V; trace e, 2,880 ML, 12 V. Partial 1/3 to 1/2 voltage drop at lower temperatures than 150 K are due to D defects moving away from hydronium ions and then through the film. That trace e fits neatly into the family shows that there is a field effect at work, not just a thickness effect.

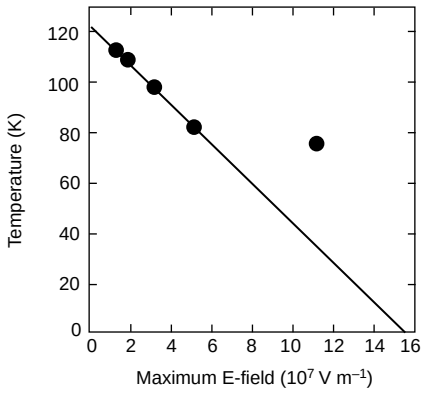

Figure 4 Hydrogen-bond defect motion versus electric field. Temperature for half-height of first voltage fall (hydrogen D-defect motion) of Fig. 3 data is plotted versus field strength. Linear fit has zero-field intercept of 124 K, and slope of -8.1×10^7 K V^{-1} m.

© 1999 Macmillan Magazines Ltd

where q_e is the electron charge. This is because their diffusion through a distance r 'flips' water dipoles over their entire path, creating a total dipole field change of $\pm(0.38\,q_e)r$ (ref. 1). Thus a D defect reduces the field by 0.38 of the initial value as they traverse the film. Only D defects move; the field polarity keeps any negative-like L defects at the film top.

Figure 3 shows the shapes of the ΔV versus T curves for a variety of field strengths, $(1.1–11) \times 10^7\,V\,m^{-1}$. These fields are weak compared to electrochemical fields ($>10^9\,V\,m^{-1}$), and are comparable to those around ions in solution. The first voltage drop moves to much lower temperatures as the strength is increased: the D-defect drift velocity is not simply proportional to field strength. The field must lower the activation barrier for motion. The first-drop temperatures from Fig. 3 are plotted against field strength in Fig. 4; four points fall on a line. The fifth point corresponds to the highest field, which probably permitted ion motion *during* ion deposition. The zero-field limit is 124 K, in agreement with previous work for mobilization of pre-existing defects[22]. The D-defect mobility temperature falls to 0 K at an extrapolated field of $16 \times 10^7\,V\,m^{-1}$. This is the field at 17 Å from a singly charged ion in water, before solvation via reorientation occurs ($\epsilon = 3.2$). Thus an ion may be able to induce rapid D-defect migration as far away as 17 Å, greatly facilitating its solvation. Theoretical estimates of this field effect do not to our knowledge exist[23].

The work reported here suggests the need to refine the physical model of water ice. □

Received 19 October 1998; accepted 20 January 1999.

1. Hobbs, P. V. *Ice Physics* (Clarendon, Oxford, 1974).
2. Whalley, E., Jones, S. J. & Gold, L. W. (eds) *Physics and Chemistry of Ice* (Royal Soc. Canada, Ottawa, 1973).
3. Pomes, R. & Roux, B. Structure and dynamics of a proton wire: A theoretical study of H^+ translocation along the single-file water chain in the gramicidin A channel. *Biophys. J.* **71,** 19–39 (1996).
4. Bainco, R., Gertner, B. J. & Hynes, J. T. Proton transfer reactions at the surface of ice. Heterogeneous reactions involved in stratospheric ozone deletion. *Ber. Bunsenges. Phys. Chem.* **102,** 518–526 (1998).
5. Eckener, U., Helmreich, D. & Engelhardt, H. in *Physics and Chemistry of Ice* (eds Whalley, E., Jones S. J. & Gold, L. W.) 242–245 (Royal Soc. Canada, Ottawa, 1973).
6. Petrenko, V. F. & Maeno, N. Ice field transistor. *J. de Phys. C* **48,** 115–119 (1987).
7. Petrenko, V. F. *Electrical Properties of Ice* (Spec. Rep. 93-20, US Army Cold Regions Research and Engineering Laboratory, Hanover, NH, 1993).
8. Collier, W. B., Ritzhaupt, G. & Devlin, J. P. Spectroscopically evaluated rates and energies for proton transfer and Bjerrum defect migration in cubic ice. *J. Phys. Chem.* **88,** 363–368 (1984).
9. Wooldridge, P. J. & Devlin, J. P. Proton trapping and defect energetics in ice from FT-IR monitoring of photoinduced isotopic exchange of isolated D_2O. *J. Chem. Phys.* **88,** 3086–3091 (1988).
10. von Hipple, A., Runck, A. H. & Westphal, W. B. in *Physics and Chemistry of Ice* (eds Whalley, E., Jones, S. J. & Gold, L. W.) 236–241 (Royal Soc. Canada, Ottawa, 1973).
11. Tsekouras, A. A., Iedema, M. J., Ellison, G. B. & Cowin, J. P. Soft-landed ions: a route to ionic solution studies. *Int. J. Mass Spectrom. Ion Proc.* **174,** 219–230 (1998).
12. Kleyn, A. W. Ion-surface interactions—from channelling to soft-landing. *Science* **275,** 1440–1441 (1997).
13. Miller, S. A., Luo, H., Pachuta, S. J. & Cooks, R. G. Soft-landing of polyatomic ions at fluorinated self-assembled monolayer surfaces. *Science* **275,** 1447–1450 (1997).
14. Engelhardt, H. in *Physics and Chemistry of Ice* (eds Whalley, E., Jones, S. J. & Gold, L. W.) 226–235 (Royal Soc. Canada, Ottawa, 1973).
15. Pfeifer, R. & Hertz, H. G. Activation energies of the proton-exchange reactions in water measured with the 1H-NMR spin echo technique. *Ber. Bunsenges. Phys. Chem.* **94,** 1349–1355 (1990).
16. Strongin, D. R., Mowlem, J. K., Lynne, K. G. & Kong, Y. Efficient magnetic focusing of low-energy ions (1–5 eV) onto solids for use in surface chemistry studies. *Rev. Sci. Instrum.* **63,** 175–188 (1992).
17. Tsekouras, A. A., Iedema, M. J. & Cowin, J. P. Soft-landed ion diffusion studies on vapor-deposited hexane films. *J. Phys. Chem.* (submitted).
18. The KP5000 system (McAllister Technical Services, Coer d'Alene, Idaho 83815, USA).
19. Materer, N. *et al.* Molecular surface structure of ice (0001): dynamical low-energy electron diffraction, total-energy calculations and molecular dynamics simulation. *Surf. Sci.* **381,** 190–210 (1997).
20. Tuckerman, M., Laasonen, K., Sprik, M. & Parrinello, M. *Ab initio* molecular dynamics simulation of the solvation and transport of hydronium and hydroxyl ions in water. *J. Chem. Phys.* **103,** 150–161 (1995).
21. Kunst, M. & Warman, J. M. Nanosecond time-resolved conductivity studies of pulse ionized ice. 2. The mobility and trapping of protons. *J. Phys. Chem.* **87,** 4093–4095 (1983).
22. Johari, G. P. & Jones, S. J. Study of the low-temperature "transition" in ice 1 h by thermally stimulated depolarization measurements. *J. Chem. Phys.* **62,** 4213–4223 (1975).
23. Hermansson, K. & Ojamäe, L. On the role of electric fields for proton transfer in water. *Solid State Ionics* **77,** 34–42 (1995).

Supplementary Information is available on *Nature*'s World-Wide Web site (http//www.nature.com) or as paper copy from the London editorial office of *Nature*.

Acknowledgements. We thank S. E. Barlow for advice. This work was conducted in the Environmental Molecular Sciences Laboratory, a collaborative users' facility of the US Department of Energy (DOE), under the Office of Biological and Environmental Research, and was supported by the Division of Chemical Sciences, US DOE. Pacific Northwest National Laboratory is operated by Battelle Memorial Institute for the US DOE.

Correspondence and requests for materials should be addressed to J.P.C. (e-mail: jp.cowin@pnl.gov).

Electrical conduction through DNA molecules

Hans-Werner Fink & Christian Schönenberger

Institute of Physics, University of Basel, Klingelbergstrasse 82, CH-4056 Basel, Switzerland

The question of whether DNA is able to transport electrons has attracted much interest, particularly as this ability may play a role as a repair mechanism after radiation damage to the DNA helix[1]. Experiments addressing DNA conductivity have involved a large number of DNA strands doped with intercalated donor and acceptor molecules, and the conductivity has been assessed from electron transfer rates as a function of the distance between the donor and acceptor sites[2,3]. But the experimental results remain contradictory, as do theoretical predictions[4]. Here we report direct measurements of electrical current as a function of the potential applied across a few DNA molecules associated into single ropes at least 600 nm long, which indicate efficient conduction through the ropes. We find that the resistivity values derived from these measurements are comparable to those of conducting polymers, and indicate that DNA transports electrical current as efficiently as a good semiconductor. This property, and the fact that DNA molecules of specific composition ranging in length from just a few nucleotides to chains several tens of micrometres long can be routinely prepared, makes DNA ideally suited for the construction of mesoscopic electronic devices.

The physical meaning of conductivity implies that there are free charge carriers available that can move under ordinary thermal conditions. This quantity is not directly accessible from measurements of the transfer rates of injected hot electrons. The simplest

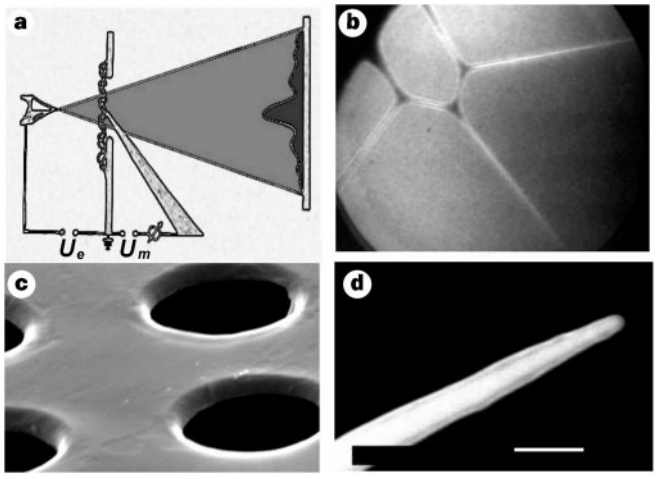

Figure 1 The low-energy electron point source (LEEPS) microscope used to investigate the conductivity of DNA. **a**, The atomic-size electron point source is placed close to a sample holder with holes spanned by DNA molecules. Due to the sharpness of the source and its closeness to the sample, a small voltage U_e (20–300 V) is sufficient to create a spherical low-energy electron wave. The projection image created by the low-energy electrons is observed at a distant detector. Between sample holder and detector, a manipulation-tip is incorporated (see text for details). This tip is placed at an electrical potential U_m with respect to the grounded sample holder and is used to mechanically and electrically manipulate the DNA ropes that are stretched over the holes in the sample holder. **b**, A projection image of λ-DNA ropes spanning a 2-μm-diameter hole. The kinetic energy of the imaging electrons is 70 eV. **c**, SEM image, showing the sample support with its 2-μm-diameter holes. **d**, SEM image of the end of a tungsten manipulation-tip used to contact the DNA ropes. Scale bar, 200 nm.

© 1999 Macmillan Magazines Ltd